Benchmarking trapped proton specification models along an EOR orbit

Sébastien Bourdarie, Pablo Caron, Marine Ruffenach, Francoise Bezerra, Robert Ecoffet

Benchmarking trapped proton specification models along an EOR orbit

S. Bourdarie, P. Caron, M. Ruffenach, F. Bezerra, R. Ecoffet

Abstract: **Eutelsat 7C (E7C), a telecommunication spacecraft, was launched on 21st of June 2019 and reached geostationary (GEO) orbit four months later after a quasi-equatorial electric orbit raising (EOR) phase. An ICARE-NG (Influence sur les Composant Avancés des Radiations de l'Espace, Nouvelle Génération) radiation monitor was implemented on the spacecraft allowing measurements of electron and proton flux as well as Single Event Upset (SEU) effect affecting various static random access memories (SRAMs) and dynamic random access memories (DRAMs). According to the cruise to GEO profile, two phases could be deduced, a first one where SEU events are dominated by trapped protons and a second one where they are attributed to cosmic rays and solar proton events. In this paper, SEU events attributed to trapped particles as well as proton flux recorded by ICARE-NG are used to benchmark proton specification models, Aerospace Proton version 8 (AP8), Aerospace Proton version 9 (AP9) and Global Radiation Earth ENvironment-proton (GREEN-p). Although, the 3D shielding of the spacecraft and payload is considered to transport accurately the proton environment down to the chip, ground tests to define cross section were not reliable enough to draw clear conclusion on specification model performances along EOR orbits.**

I. Introduction

Although specification models for trapped electrons and protons in the Earth space environment have been widely benchmarked along very popular orbits, i.e. GEOstationary (GEO) [1]-[3], Low Earth Orbit (LEO) [2]-[6], and to some extent, navigation orbits, there is a clear gap in between like along Electrical Orbit Raising (EOR) phase to reach GEO. Recently, it was found that AP8 [7] and AP9 [8] were underestimating trapped proton flux in the range 4 to 10 MeV from 5000 km to 20 000 km altitudes [9], but no benchmarking of energetic trapped proton specification were conducted above 1500 km with radiation induced effects such as SEU events.

An ICARE-NG (Influence sur les Composant Avancés des Radiations de l'Espace, Nouvelle Génération) radiation monitor has been implemented on the Eutelsat 7° number C (E7C) spacecraft launched on 21st June 2019. The spacecraft reached GEO following a 4 months EOR phase. During the entire crossing of the radiation belts, the ICARE-NG instrument provided electron and proton flux measurement [10] respectively in the range 1.45 to 2.0 MeV and 50 to 141 MeV. On the same instrument, an electronic test board (MEX) is implemented were radiation effects are collected [11]. In particular, SEU events are recorded on different chips. These in-situ measurements are considered here to benchmark proton specification models, AP8 min, AP9 V1.50.001 Mean, and GREEN-p (Global Radiation Earth ENvironment-proton) [12].

Section II describes E7C's EOR orbit and in-situ measurements of interest. Section III details the SEU predictions out of specification models along E7C's EOR orbit. Those predictions are compared to in-flight data and results are then discussed. To complete the previous analysis, proton flux predictions from specification models along E7C's orbit are compared to measurements from ICARE spectrometers in section IV. Finally, in Section V conclusions are drawn on the performances of AP8 min, AP9 V1.50.001 Mean and GREEN-p to reproduce in-flight observations along an EOR orbit.

II. Flight Data

E7C is a spacecraft that reached its final station at GEO with electrical orbit raising (EOR). It was launched on June 21st, 2019 from Kourou, French Guyana. The cruise to GEO lasted for about 4 months. The evolution of perigee, apogee, and inclination from launch date to end of October 2019 is given in Fig.1. The spacecraft left the energetic proton belt in about 1.5 month of mission (perigee at 5 000 km 1 month after launch and at 10000 km 2 months after launch).

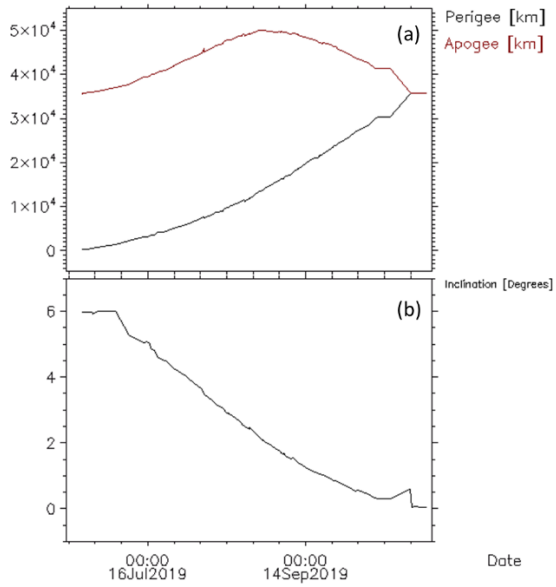

Fig. 1 E7C orbital parameters out of Two Lines Elements versus time during EOR phase to GEO, with apogee-perigee (a) and inclination (b).

This work was supported by CNES R&T program.

S. Bourdarie and Pablo Caron are with ONERA The French aerospace lab/Département Environnement Spatial, 31400 Toulouse France (telephone; +33-562-2756, e-mail: Sebastien.Bourdarie@onera.fr).

F. Bezerra, R. Ecoffet and M. Ruffenach are with CNES, 18 av. E. Belin 31401 Toulouse, France

On the MEX experiment, two memories are of particular interest because they have been fully calibrated at ground under a proton beam: the cumulated SEU collected along E7C EOR phase to GEO are given in Fig. 2. Because their respective proton cross sections are not the same [13], different slopes in the curves are found, 0.95 SEU/day for the Samsung K7A801800M SSRAM and 4.3 SEU/day for IDT IDT71V3558S SSRAM while E7C was still crossing the trapped proton belt. After E7C perigee was definitively above the trapped energetic proton belt, the SEU rates became respectively 0.06 SEU/day and 0.19 SEU/day. Those events can be attributed to galactic cosmic rays with no doubt because the spacecraft was above the proton belt, and no solar energetic particles were observed during this time. Assuming the SEU rate due to galactic cosmic rays is the same while E7C is in the trapped proton radiation belt, the SEUs only attributed to trapped proton can be deduced. To this end, an average SEU rate of 0.06 SEU per day for the Samsung K7A801800M SSRAM and 0.19 SEU per day for IDT IDT71V3558S SSRAM is subtracted from the total number of SEUs recorded by ICARE-NG. The total number of SEUs with or without the galactic cosmic ray contribution are compared in Fig.3. When E7C does not cross the trapped proton belt anymore, because the perigee is high enough, the total SEU number only attributed to trapped proton does not evolve anymore.

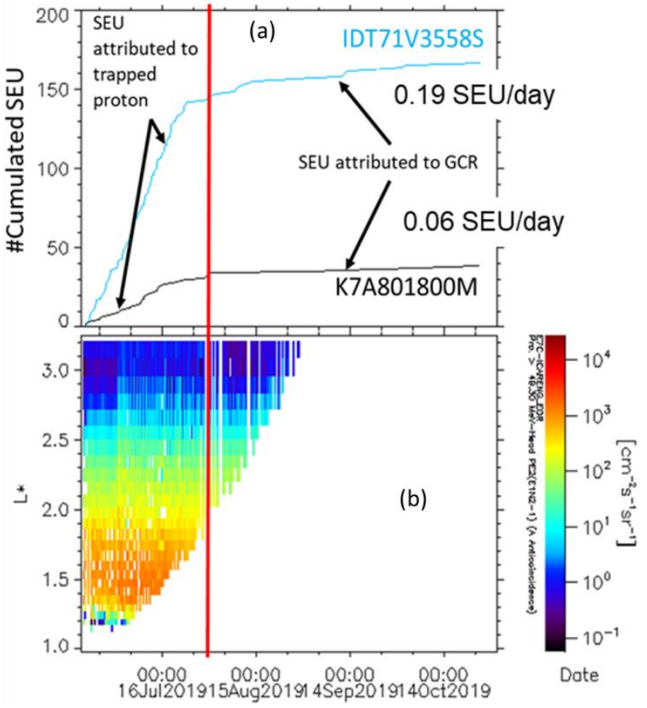

Fig. 2 Top panel (a) - Cumulated SEU event collected from two chips during E7C's EOR phase to GEO. Bottom panel (b) – >49.3 MeV trapped proton flux measurements from ICARE-NG payload onboard E7C.

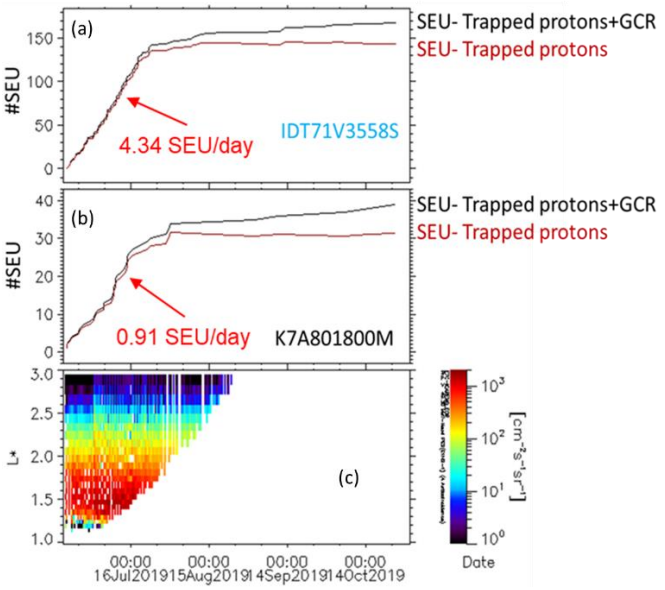

Fig. 3 Top panels (a and b)- Accumulated SEU events collected from two chips, IDT71V3558S (a) and K7A801800M (b) during E7C's EOR phase to GEO with and without galactic cosmic ray contribution. Bottom panel (c) – >49.3 MeV trapped proton flux measurements from ICARE-NG payload onboard E7C.

We can conclude that a minimum of 93.7% of SEU events recorded on the Samsung K7A801800M SSRAM and 95.6% of SEU events recorded on the Samsung IDT71V3558S SSRAM can be attributed to trapped protons when E7C perigee is still in the energetic proton belt. Only the data where the contribution from galactic cosmic rays is removed will be used next.

III. SEU PREDICTIONS OUT OF SPECIFICATION MODELS

A. *Approach*

To perform SEU event predictions affecting the two chips from specification models, AP8 min with ESA interpolations [7], AP9 V1.50.001 Mean [8], and GREEN-p [12], the following strategy is applied (similar to [14], [15]):

- E7C trajectory is computed with a time step of 20s using the Simplified General Perturbation version 4 model, SGP4 [16], to propagate Two Line Elements, TLE, collected on Space-track [17].
- A proton differential spectrum is deduced at each orbital locations (every 20s) from AP8 min with ESA interpolation, AP9 V1.50.001 Mean, and GREEN-p models.
- At each new increment of SEUs collected by the ICARE-NG MEX board, the proton differential fluence is calculated from the switch-on of the instrument to the time of the new event.
- Each proton differential fluence is transported down to the chip accounting for the 3D shielding from the payload and the spacecraft around it. Note that it allows us to account for highly anisotropy of the shielding distribution.
- The cumulated SEU events are deduced by multiplying the transported fluence with the chip's proton cross section.

Propagating the proton fluence down to the chips requires a good knowledge of the 3D shielding surrounding them. To do so, the distribution of shielding thicknesses seen by the SRAM devices was calculated by a sector analysis carried out by MAXAR Company using the FASTRAD software [18]. The 3D CAD model of the spacecraft is then simplified to the distribution of shielding in the 4π steradians obtained with FASTRAD. From GEometry ANd Traking toolkit (GEANT-4) [19] the matrix (Fig. 4) to transport a spectrum outside E7C down to the chip can be computed considering the 3D sector analysis. It is found that protons with energy less than 30 MeV outside the spacecraft cannot reach the SRAMs.

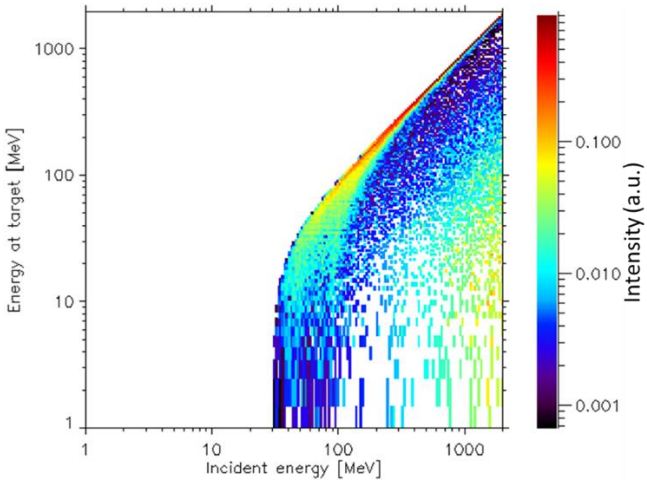

Fig. 4 Conversion matrix from incident proton energy to transmitted proton energy considering E7C 3D shielding.

B. *Device cross sections*

A good definition of the proton device cross section is also crucial to get accurate SEU predictions. Only two parts per memory of interest were tested in years 2000s at the University Catholic of Louvain (UCL) proton beam [20]. It can be noticed that the results obtained from one part to another present significant differences (Fig. 5). Moreover, the authors of [20] specifies that the tests did not make it possible to define the threshold energy given that the UCL accelerator cannot reasonably go below 9 MeV. The lack of statistics (number of parts tested limited to two) and the indeterminacy of the threshold energy leave many degrees of freedom to define a precise Weibull fit. To reflect these uncertainties, several cross section curves have been defined (Fig. 5 and Table I):

- Xsection 1: Same as [13], threshold energy set at 9 MeV and saturation cross section close to a worst case given the dispersion of the experimental points.
- Xsection 2: Threshold energy set at 9 MeV and curve passing through the lowest points (most optimistic cross section).
- Xsection 3: Threshold energy set at 5 MeV and curve passing through the highest points (worst-case cross section).

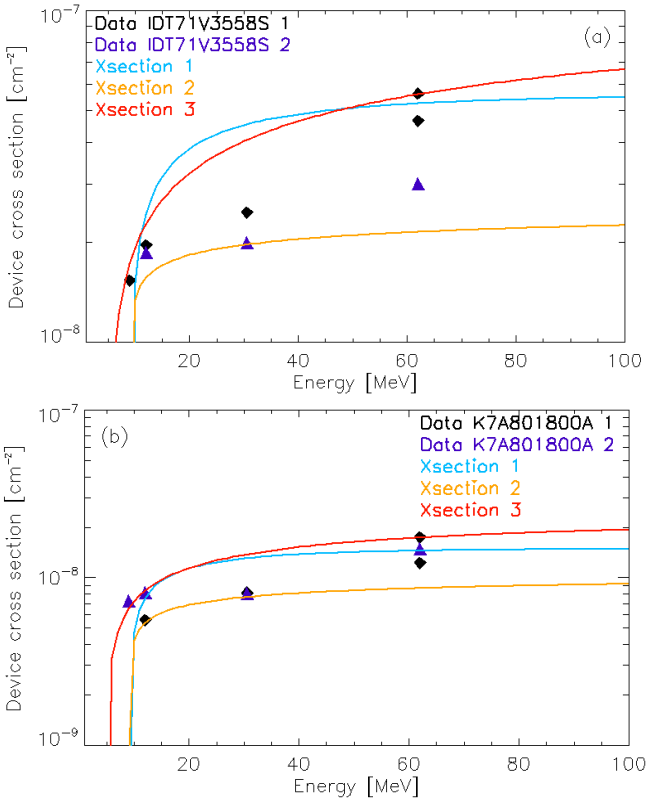

Fig. 5: Device cross sections for protons (top (a) is for IDT IDT71V3558S and bottom (b) is for Samsung K7A801800A

TABLE I. WEIBULL FIT PARAMETER FOR THE PROTON DEVICE CROSS SECTION

		Eth [MeV]	σ_{sat} [cm^{-2}]	W	S
IDT71V3558S	X section 1	9	5.64×10^{-8}	8.66	0.54
	X section 2	9	2.82×10^{-8}	8.66	0.2
	X section 3	5	1.07×10^{-7}	100.	0.54
K7A801800A	X section 1	9	1.5×10^{-8}	5.8	0.55
	X section 2	9	1.07×10^{-8}	10	0.3
	X section 3	5	2.25×10^{-8}	28	0.55

C. *Environment calculations at the chip*

The average fluxes of trapped protons encountered by E7C during the EOR phase predicted by the AP8 min, AP9 V1.50.001 Mean, GREEN-p models, and measured by ICARE-NG are compared in Fig. 6. The ICARE-NG spectrum is deduced from integrated proton channels because these measurements are omnidirectional unlike differential channel ones. The average integrated spectrum, which covers the energy range 49 MeV-121 MeV, is then approximated by an exponential spectrum which will be derived to obtain the curve presented here. This spectrum is extrapolated for energies below 49 MeV and above 121 MeV. Resulting flux in this energy range must be considered with great caution. Note that the range of interest, given the transfer function (Fig. 4) and the sensitivity of the components (Fig. 5), is 30 MeV to around 100-200 MeV. Beyond that, the fluxes are weak and the protons will have a minor influence on the total number of single events.

In the 30-150 MeV range, we notice that the models or measurements are relatively close, AP9 V1.50.001 producing

the highest fluxes while GREEN-p predicts the lowest ones. AP8 min and ICARE-NG measurements predict intermediate flux levels.

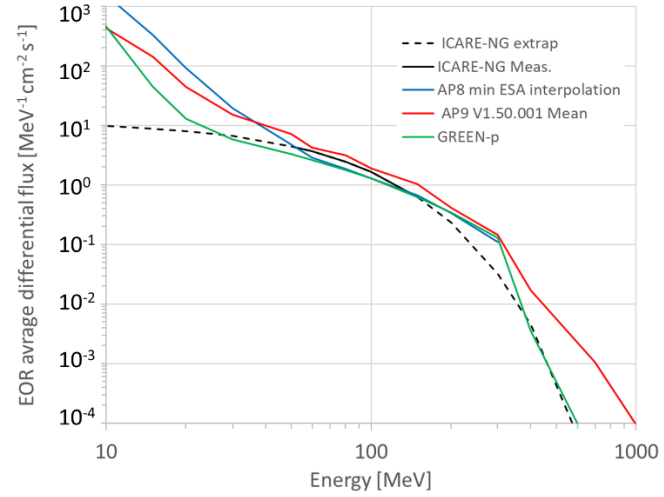

Fig. 6: Comparison of the differential fluxes of trapped protons averaged over the entire EOR phase of E7C predicted by the AP8min, AP9 V1.50.001 Mean, and GREEN-p specification models as well as restored from the measurements of the ICARE-NG monitor

These spectra are then transported to the chip by applying the transfer matrix (Fig. 4). The comparison of proton fluxes transmitted at the chip level is shown in Fig. 7. Consistent with previous findings, AP9 V1.50.001 Mean provides the highest predictions while GREEN-p predicts the lowest transmitted fluxes.

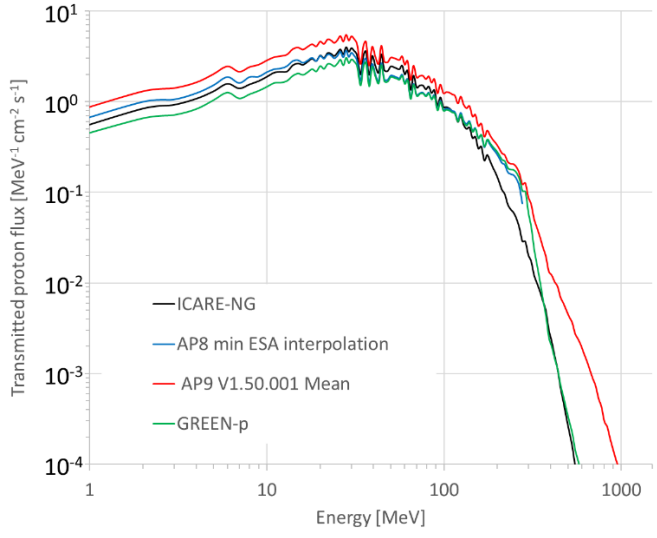

Fig. 7 Comparison of the differential fluxes of protons transmitted to the chip of the MEX board and averaged over the entire EOR phase of E7C predicted by the AP8min, AP9 V1.50.001 Mean, and GREEN-p specification models as well as restored from the measurements of the ICARE- NG monitor.

D. Results

Finally, the total fluence (transmitted to the chip) from launch time to each time a new SEU is recorded is convolved with the sensitivity curve of each memory in order to obtain a forecast of the total number of SEUs induced by the trapped protons (Fig. 8 and Fig. 9). In order to analyze the prediction impacts of SEU induced by the uncertainty in the definition of the cross section curve, three sensitivity curves are used (X section 1, X section 2 and X section3), the envelope of the cross section being given by X section 2 (minimum value) and X section 3 (maximum value).

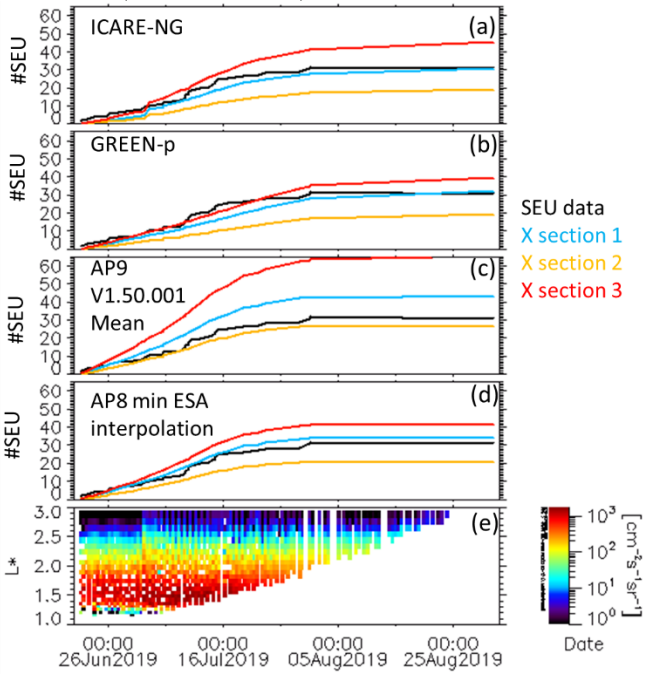

Fig. 8 Top four panels: cumulated number of SEUs predicted from ICARE-NG (a), GREEN-p (b), AP9 V1.50.001 Mean (c) and AP8 min (d) and compared with ICARE-MEX measurements during the E7C's EOR phase on the Samsung K7A801800A memory. Bottom panel (e): L* versus time color map of > 49.3 MeV proton flux measured by ICARE-NG on board E7C.

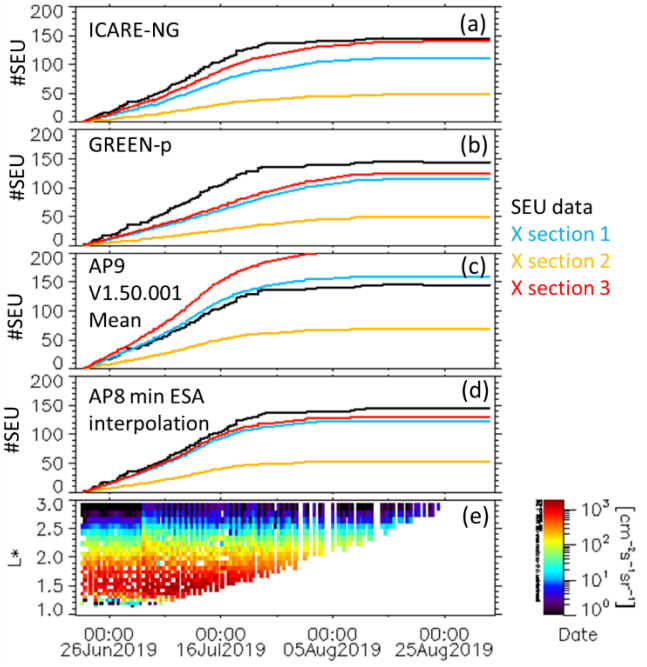

Fig. 9 Top four panels: cumulated number of SEUs predicted from ICARE-NG (a), GREEN-p (b), AP9 V1.50.001 Mean (c) and AP8 min (d) and compared with ICARE-MEX measurements during the E7C's EOR phase on the IDT IDT71V3558S memory. Bottom panel (e): L* versus time color map of > 49.3 MeV proton flux measured by ICARE-NG on board E7C.

In the case of the Samsung K7A801800A memory, in flight measurements are systematically between the maximum

predicted value (X section 3) and the minimum predicted one (X section 2) regardless of the model used (AP8min, AP9 V1.50.001 Mean, GREEN-p) or ICARE-NG measurements (Fig. 8). The best performance is obtained with AP8min X section 1, AP9 V1.50.001 Mean X section 2, GREEN-p X section 3 and ICARE-NG X section 1. In other words, AP9 V1.50.001 Mean is close to in-flight observations if we consider the weakest cross-section curve: AP9 V1.50.001 Mean would, therefore, tend to overestimate the observations made with the Samsung memory. On the other hand, GREEN-p is close to in-flight observations if we consider the strongest cross-section curve: GREEN-p would, therefore, tend to underestimate the observations made with the Samsung memory. AP8 min and ICARE-NG produce very close results and are in agreement with each other.

In the case of the IDT IDT71V3558S memory, the situation is quite different and not necessarily consistent with the results obtained previously (Fig. 9). The in-flight measurements are only between the maximum predicted value (X section 3) and the minimum predicted value (X section 2) with AP9 V1.50.001 Mean. AP8 min and GREEN-p underestimate in-flight measurements regardless of the defined cross-section curve. More surprisingly, the predictions deduced from the ICARE-NG measurements underestimate the in-flight measurements whatever the defined cross-section curve. It should, however, be remembered that the proton spectrum deduced from the ICARE-NG measurements underestimate the proton fluxes for energies below 50 MeV and for energies above 120 MeV.

Note that in all calculations the proton environment is assumed isotropic. This assumption could also lead to some additional uncertainty in the SEU rates evaluation. Nevertheless, the anisotropy of the proton environment is decreasing with altitude. Whereas it is proven to be large for altitudes below 1000 km, it is almost negligible above [21]. As a result, the proton peak flux encountered by E7C being about at 2800 km altitude it is expected that the isotropy of the proton flux assumption is not affecting the results.

SEU rates measured and predicted by the specification models are compared in TABLE II considering 3 cross section curves for each of the memories. Ratios deduced between forecasts and measurements (last two columns) are color coded: green if the ratio is between 0.8 and 1.2, orange if the ratio is between (0.5 and 0.8) and (1.2 and 2), and red if the ratio is less than 0.5 or greater than 2. These results cover the period 21 June-17 July 2019. In view of the comparisons obtained for the two chips, it is extremely difficult to draw clear conclusions as to the performance of the specification models for an EOR orbit (TABLE II.). We can identify a trend but it should be taken with great caution:

- GREEN-p seems to underestimate the fluxes of trapped protons.
- AP9 V1.50.001 seems to overestimate trapped proton fluxes.
- AP8 min seems to produce the best predictions.

TABLE II. SEU RATES MEASURED AND PREDICTED BY THE SPECIFICATION MODELS.

	X section	Samsung: SEU/day	IDT SEU/day	Samsung : Ratio to flight data	IDT Ratio to flight data
Data		0.907	4.338		
AP8 min	1	1.066	3.897	1.18	0.9
	2	0.653	1.676	0.72	0.39
	3	1.299	4 .132	1.43	0.95
AP9 V1.50.001 Mean	1	1.323	4.909	1.46	1.13
	2	0.824	2.113	0.91	0.49
	3	1.962	6.341	2.16	1.46
GREEN-p	1	0.68	2.494	0.75	0.57
	2	0.419	1.066	0.46	0.25
	3	0.856	2.777	0.94	0.64
ICARE-NG	1	0.83	2.939	0.92	0.68
	2	0.512	1.258	0.56	0.29
	3	1.216	3.709	1.34	0.86

IV. Comparison of ICARE-NG measurements with specification models

To go beyond previous conclusions, comparisons were made between ICARE-NG measurements and predictions of the fluxes of trapped protons obtained with the AP8 min, AP9 V1.50.001 Mean, and GREEN-p models. To do so, each time ICARE-NG measurements are above the background noise of the radiation monitor, a forecast is made with the each specification models, AP8 min, AP9 V1.50.001 Mean, and GREEN-p. Only the energy-integrated proton channels have been considered because these measurements are omnidirectional, unlike the differential ones, which have more "directionality" in the measurement and thus make it possible to avoid any potential bias linked to a potentially highly anisotropic environment. In Fig. 10 the fluxes predicted by the specification models at the E7C measurement locations are compared with the ICARE-NG measurements for three channels, >49.3, >79.36 and >121.6 MeV. To interpret these graphs, it is important to keep in mind that we are comparing fluxes averaged over long periods of time (AP8 min = several years, AP9 = more than one solar cycle, and GREEN-p = 1 year) with instantaneous proton fluxes (ICARE-NG measurements accumulation time is 8s).

From these comparisons, it turns out that AP8 min perfectly reproduces large fluxes (peak of the proton belt in the region 1.1<R<1.9). On the other hand, it is clear that AP8 min underestimates the proton fluxes in the outer region of the proton belt (R> 1.9) because the proton belt is more extended towards high altitudes than predicted by AP8 min. The fact that AP8 min reproduces large fluxes quite faithfully reinforces its good behavior in terms of SEU forecasting, with weak fluxes having little impact on the results.

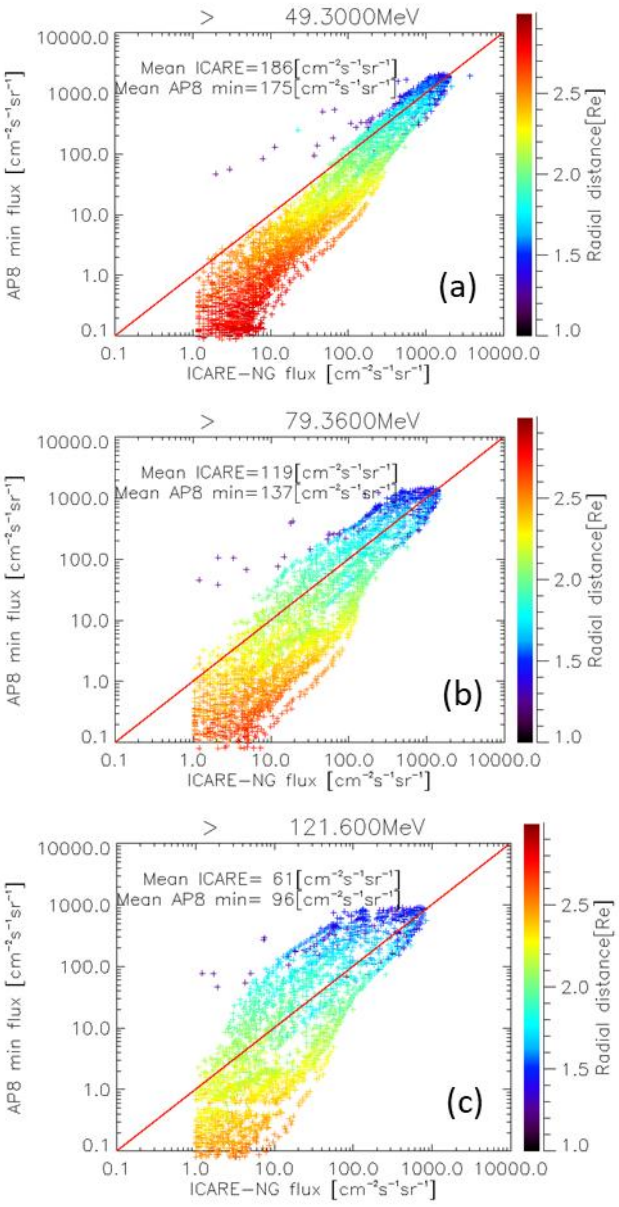

Fig. 10 Comparison of ICARE-NG measurements with AP8 min model ((a) is for > 49.3 MeV, (b) is for > 79.36 MeV and (c) is for >121.6 MeV. The color code indicates the radial distance in Earth radii of E7C satellite.

AP9 V1.50.001 Mean also reproduces the large fluxes of trapped protons quite faithfully with a tendency to overestimate more and more in-situ measurements as the energy increases. In the outer zone of the proton belt, AP9 V1.50.001 Mean overestimates the fluxes of trapped protons: the proton belt seen by AP9 is significantly larger than shown by the ICARE-NG measurements. This observation is consistent with the conclusions obtained with the SEU calculations.

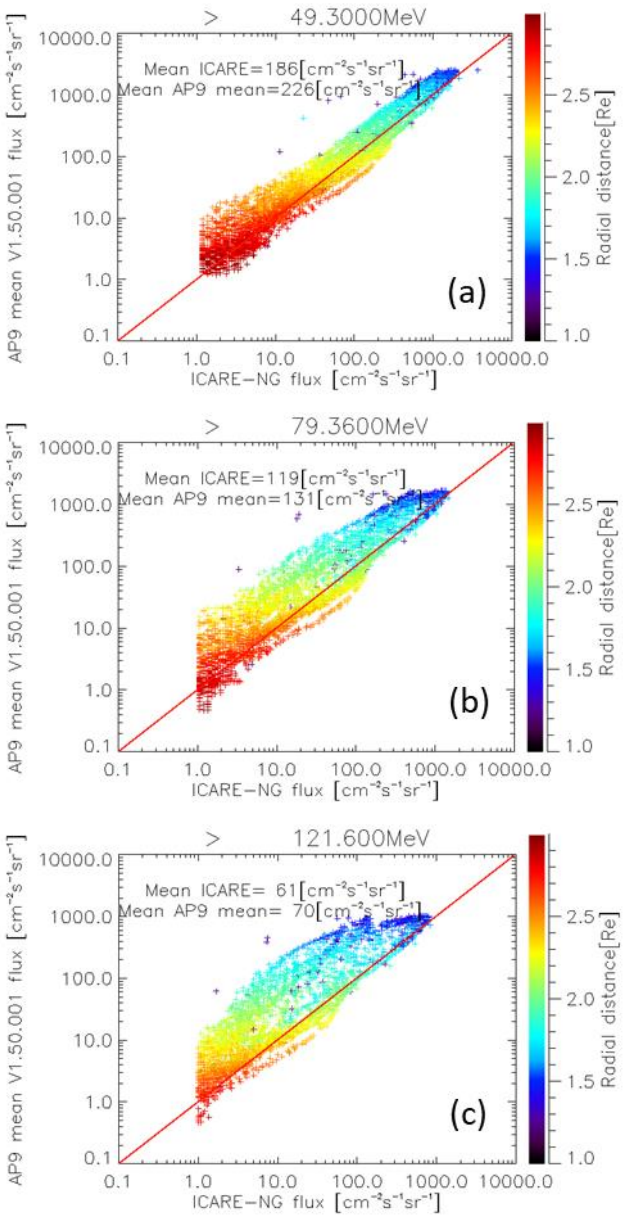

Fig. 11 Comparison of ICARE-NG measurements with AP9 V1.50.001 Mean model ((a) is for > 49.3 MeV, (b) is for > 79.36 MeV and (c) is for >121.6 MeV. The color code indicates the radial distance in Earth radii of E7C satellite.

GREEN-p systematically underestimates the peak flux of trapped protons at all energies. On the other hand, GREEN-p greatly overestimates the proton fluxes trapped in the outer region of the proton belt because the proton belt seen by GREEN-p is too extended in altitude. The underestimation of the peak flux is consistent with the SEU forecast results. The rather consequent overestimation of fluxes in the outer region tends to compensate on average for this bias, which makes it possible to obtain SEU forecasts relatively close to in-flight measurements.

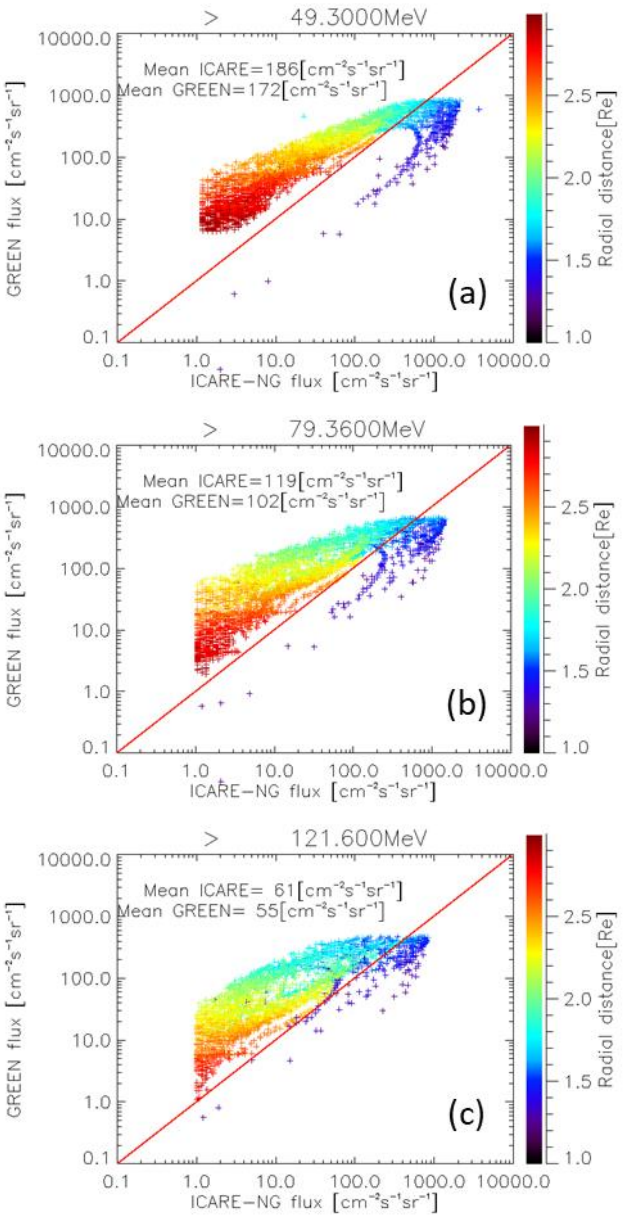

Fig. 12 Comparison of ICARE-NG measurements with GREEN-p model (top is for > 49.3 MeV, middle is for > 79.36 MeV and bottom is for >121.6 MeV. The color code indicates the radial distance in Earth radii of E7C satellite.

V. Conclusions

The analysis of the SEU measurements on the Samsung and IDT memories and their comparison with the predictions made with the trapped proton specification models, AP8 min, AP9 V1.50.001 Mean, and GREEN-p does not make it possible to define with no doubt which is the most efficient model for EOR type orbits. The comparisons obtained from one memory to another are not perfectly consistent. This is probably linked to too large uncertainties in the proton cross-section curves obtained from ground tests. In view of all the results, the AP8 min model seems to provide the predictions most in agreement with the E7C-ICARE-NG-MEX measurements while AP9 V1.50.001 tends to slightly overestimate them and GREENp slightly underestimate them.

The comparison of the average fluxes predicted by the specification models with the instantaneous flux measurements from the ICARE-NG monitor on board E7C provides additional information. The peak flux is well reproduced by the AP8 min and AP9 V1.50.001 Mean models while GREEN-p underestimates it. On the other hand, the models all fail in the outer zone of the proton belt where fluxes are lower.

These results seem to confirm that the AP8 min model is the most realistic one, even if not perfect, for an EOR orbit such as E7C.

V. Acknowledgments

The authors wish to thanks the CNES R&T program for their full support to this activity. The authors would like to thank EUTELSAT and MAXAR for the CARMEN4 flight opportunity.

VII. References

[1] M. Pinto, J.M. Sampaio, L. Arruda, P. Gonçalves, P. Ribeiro, T. Sousa, et al., "CTTB Memory Test Board Single Event Effect Geostationary in-flight Data Analysis," 2020 20th European Conference on Radiation and Its Effects on Components and Systems (RADECS), Toulouse, France, 2020, pp. 165-170, doi: 10.1109/RADECS50773.2020.9857705.

[2] D. L. Hansen, S. Resor, B. Vermeire, and D. Czajkowski, "Comparison of Figure of Merit Calculations to On-Orbit Data," 2023 IEEE Radiation Effects Data Workshop (REDW) (in conjunction with 2023 NSREC), Kansas City, MO, USA, 2023, pp. 234-241, doi: 10.1109/REDW61050.2023.10265844.

[3] D. L. Hansen, K. Jobe, J. Whittington, M. Shoga, and D. A. Sunderland, "Correlation of Prediction to On-Orbit SEU Performance for a Commercial 0.25- µ m CMOS SRAM," in IEEE Transactions on Nuclear Science, vol. 54, no. 6, pp. 2525-2533, Dec. 2007, doi: 10.1109/TNS.2007.908787.

[4] C. Poivey, R. Harboe-Sorensen, M. Pinto, M. Poizat, N. Fleurinck, K. Grürmann, et al., "SEL and SEU In-flight data from memories on-board PROBA-II spacecrzft"AP8, 2022 IEEE Radiation Effects Data Workshop (REDW) (in conjunction with 2022 NSREC), Provo, UT, USA, 2022, pp. 94-99, doi: 10.1109/REDW56037.2022.9921736.

[5] A. L. Vampola, M. Lauriente, D. C. Wilkinson, J. Allen, and F. Albin, "Single Event Upsets correlated with environment," in IEEE Transactions on Nuclear Science, vol. 41, no. 6, pp. 2383-2388, Dec. 1994, doi: 10.1109/23.340591.

[6] Y. Kimoto, N. Nemoto, H. Matsumoto, K. Ueno, T. Goka, and T. Omodaka, "Space radiation environment and its effects on satellites: analysis of the first data from TEDA on board ADEOS-II," in IEEE Transactions on Nuclear Science, vol. 52, no. 5, pp. 1574-1578, Oct. 2005, doi: 10.1109/TNS.2005.855822.

[7] D.M. Sawyer and J.I. Vette, "AP8 trapped proton model environment for solar maximum and minimum," NSSDC/WDC-A-R&S 76-06, Natl. Space Sci. Data Cent., Greenbelt, MD, Dec. 1976.

[8] G. P. Ginet, T. P. O'Brien, S. L. Huston, W. R. Johnston, T. B. Guild, R. Friedel, and D. Madden, "AE9, AP9 and SPM: New models for specifying the trapped energetic particle and space plasma environment," The Van Allen Probes Mission, Ed. N; Fox and J.L. Burch, Springer Boston, MA., pp. 579-615, March 2013, doi: 10.1007/978-1-4899-7433-4_18.

[9] A. Brunet, A. Sicard, C. Papadimitriou, D. Lazaro, and P. Caron, "OMEP-EOR: A MeV proton flux specification model for electric orbit raising missions", J. Space Weather Space Clim., vol. 11, pp. 55, 2021, doi: https://doi.org/10.1051/swsc/2021038.

[10] P. Caron, S. Bourdarie, D. Falguère, D. Lazaro, P. Bourdoux, V. Thakur, et al., "In-Flight Measurements of Radiation Environment Observed by Eutelsat 7C (Electric Orbit Raising Satellite)," in IEEE Transactions on Nuclear Science, vol. 69, no. 7, pp. 1527-1532, Jul. 2022, doi: 10.1109/TNS.2022.3158470.

[11] F. Bezerra, M. Ruffenach, R. Ecoffet, J. Caron, J. Mekki, L. Coïc, et al., "14 years of in-flight experimental data on CARMEN-MEX," in IEEE Transactions on Nuclear Science, doi: 10.1109/TNS.2023.3246733.
[12] A. Sicard, D. Boscher, S. Bourdarie, D. Lazaro, D. Standarovski, and R. Ecoffet, “GREEN: the new Global Radiation Earth ENvironment model (beta version),” Ann. Geophys., vol. 36, no. 4, pp. 953-967, Jul. 2018, doi: 10.5194/angeo-36-953-2018.
[13] A. Varotsou, N. Chatry, P.F. Peyrard, F. Bezerra, A. Samaras, E. Lorfèvre, et al., "Shielding geometry effect on SEE prediction using the new OMERE release: JASON-2 mission case study," 2011 12th European Conference on Radiation and Its Effects on Components and Systems, Seville, Spain, 2011, pp. 849-853, doi: 10.1109/RADECS.2011.6131315.
[14] S. Bourdarie, C. Inguimbert, D. Standarovski, J.R. Vaillé, A. Sicard-Piet, D. Falguère, et al., "Benchmarking Ionizing Space Environment Models," in IEEE Transactions on Nuclear Science, vol. 64, no. 8, pp. 2023-2030, Aug. 2017, doi: 10.1109/TNS.2017.2654687.
[15] S. Bourdarie, P. Calvel, C. Barillot, L. Rey, T. Parrinello, B. Hoyos, et al., "How Much Do Solar Cycle Variations Impact Long-Term Effect Predictions at LEO?," in IEEE Transactions on Nuclear Science, vol. 67, no. 10, pp. 2196-2202, Oct. 2020, doi: 10.1109/TNS.2020.3008251.
[16] Celestrak, accessed on April 10th, 2019. [Online]. Available: http://celestrak.com/NORAD/documentation/spacetrk.pdf
[17] Space track, accessed on April 10th, 2019. [Online]. Available: https://www.space-track.org/
[18] FASTRAD, accessed on September 6th, 2019: [Online]. Available: http://www.fastrad.net/
[19] Geant-4, accessed on February 12th, 2024 : [Online]. Available : https://geant4.org/
[20] T. Nuns, D. Falguere, and S. Duzellier, "Caractérisation SEE aux ions lourds et protons de deux types de SSRAM par une interface FPGA", Rapport technique de synthèse, ONERA-DESP, 2004.
[21] G. P. Ginet, B. K. Dichter, D. H. Brautigam, and D. Madden, "Proton Flux Anisotropy in Low Earth Orbit," in IEEE Transactions on Nuclear Science, vol. 54, no. 6, pp. 1975-1980, Dec. 2007, doi: 10.1109/TNS.2007.910041.